

ECE445

Senior Design Laboratory

Design Document

Spherical Bio-Inspired Tensegrity Multiple Step Robot with LCE Actuation

Team Member:

Yiqing Xiang (yiqingx3@illinois.edu)

Ziye Chen (ziyec2@illinois.edu)

Dongzi [Li\(dongzil2@illinois.edu\)](mailto:dongzil2@illinois.edu)

Yuxuan [Huang \(yh59@illinois.edu\)](mailto:yh59@illinois.edu)

Requirement Verification

Contents

1. Introduction	3
1.1 Problem	3
1.2 Solution	4
1.3 High-Level Requirements	5
2. Design	6
2.1 Power Module	7
2.1.1 Voltage and Current Stabilization	8
2.1.2 Battery Configuration and Physical Constraints	9
2.1.3 Endurance and Operational Duration	10
2.2 Control Module	10
2.2.1 ESP32 and WiFi Implementation	11
2.2.2 UI Interface and Control System	12
2.3 Control Module	13
2.3.1 ESP32 Controller and Communication	13
2.3.2 GPIO Control and Signal Routing	15
2.3.3 Power Input and Electrical Requirement	16
2.4 Power System	错误! 未定义书签。
2.5 Schematics	错误! 未定义书签。
2.6 Driven Module	错误! 未定义书签。
2.7 Tolerance Analysis	错误! 未定义书签。
3. Cost	17
3.1 Labor Cost	23
3.1 Part Cost	24
4. Schedule	24
5. Ethics and Safety	25
5.1 Ethics & Safety Concerns	25
5.1.1 Ethics Concerns	25
5.1.2 Safety Concern	26
5.2 Addressments & Design Decisions	27
Reference	28

Requirement Verification

1. Introduction

1.1 Problem

Tensegrity-based spherical robots in this design utilize a hollow body that consists of a Tensegrity Structure (HTS) which achieves continuous rolling when the length of the connecting rods is altered, the retraction of which is usually accomplished with LCE (L) actuators. Nevertheless, some drawbacks, such as energy dependency, still exist. Conventional HTS robots are often powered by external sources, like tethered power supply, and this imposes a limit on the range of motion of the robots. On the other hand, the using of external batteries brings

Requirement Verification

about the problem of bulkiness [6]. Accordingly, system integration has emerged as one of the key areas where this research aims at improving it. Although untethered HTS robots have made some progress in removing these issues, the kind based on LCE still relies on the presence of thermal surfaces to create temperature variations [2]. With the laser driven HTS robot, apart from the problems of constant recalibration, there exist the issues of difficulty in both positioning different rods simultaneously and having sufficient control precision locally [1]. The approach of steering the robot movement is very tricky and unagile, which lacks immediate interaction response [5]; therefore, the human-robot interaction complexity remains to be dealt with as another key challenge area.

To further enhance locomotion adaptability and multi-terrain navigation, our research proposes the "Spherical Bio-Inspired Tensegrity Multiple Step Robot with LCE Actuation." Building upon the existing HTS framework, we introduce a structural and procedural upgrade by transitioning from a single-unit body to a modular, multi-unit assembly. This multiple step configuration aims to overcome the stride limitations and lack of redundancy inherent in single-unit structures. By integrating a modular control program with the PCB-LCE system, we seek to address the challenges of simultaneous rod positioning and local control precision, ultimately simplifying human-robot interaction and enabling more agile, multi-step gait patterns in complex environments.

1.2 Solution

This study proposes a Spherical Bio-Inspired Tensegrity Multiple Step Robot with LCE Actuation, which advances existing designs by transitioning from a standalone unit to a coordinated multi-unit system linked through specialized interconnection structures. Our solution tackles the shortcomings of current models through a highly integrated, modular framework.

First, the robot achieves full autonomy and untethered operation by embedding the battery module directly into the structure to power the PCB, effectively replacing traditional rigid rods. This integrated power system allows for simultaneous processing of power and control signals, eliminating dependency on external sources and significantly enhancing mobility autonomy.

Secondly, the actuation system leverages the thermal responsiveness of Liquid Crystal Elastomer (LCE) combined with a custom-developed serpentine conductive film and a PCB-based heating circuit. This configuration enables independent addressing or parallel control of multiple rods, facilitating seamless communication between the client (UI) and the robot servers. A computer-based graphical UI allows for precise

Requirement Verification

regulation of each rod's heating state, ensuring high user-friendliness and responsive interaction.

Crucially, this research introduces a modular upgrade by designing robust interconnection mechanisms that allow multiple tensegrity units to operate in coordination. Unlike previous single-body designs, this multi-unit approach enables "multiple step" locomotion patterns and enhanced redundant stability. By synchronizing the expansion and contraction of LCE actuators across the interconnected framework through upgraded control programs, the robot can navigate complex terrains with greater agility and structural resilience.

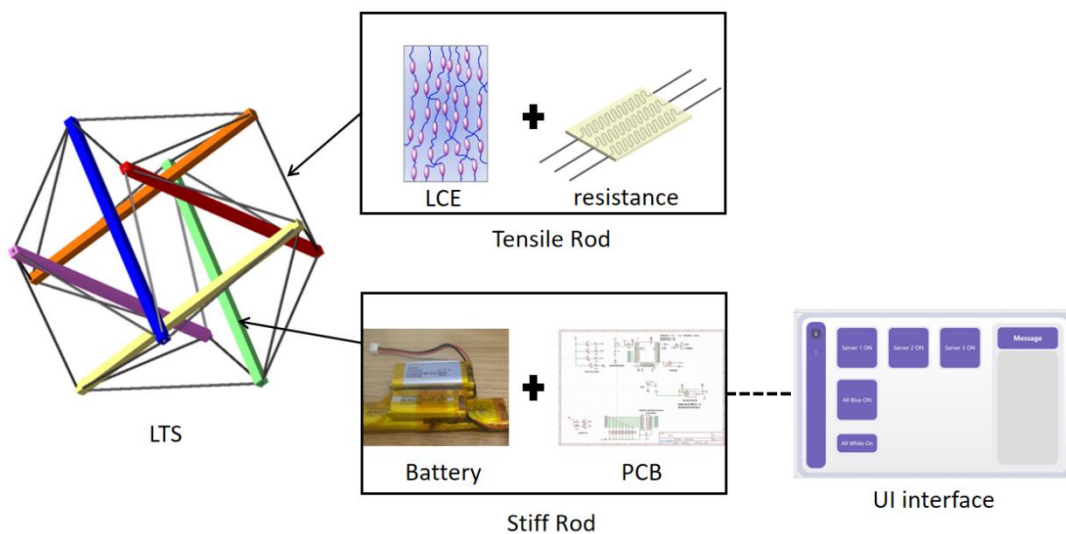


Figure 1. Visual Aid

1.3 High-Level Requirements

- i. The hard-soft hybrid structure (rigid rods connected by soft materials) must maintain stability in both static and dynamic states, with a maximum deformation of $\leq 5\%$ under a load of 1 kg applied.
- ii. The wireless control module, including the interactive UI, must achieve a signal transmission latency of ≤ 100 ms and support a control range of at least 10 meters.
- iii. The user must be able to control the robot to move in four primary directions (forward, backward, left, right) with a directional accuracy of $\pm 5^\circ$ and a minimum turning radius of 20 cm.

Requirement Verification

2. Design

The overall system is organized into four interconnected subsystems. Compared with the original single-step actuation design, this updated version emphasizes coordinated, repeatable, and time-sequenced actuation to enable continuous multi-step locomotion. Each module is described in terms of its function, design requirements, and validation approach. The complete system architecture is illustrated in the block diagram (Figure 2).

The four subsystems are:

1. Power Module: provides stable and sustained energy supply for long-duration and repeated actuation.
2. Control Module: serves as the central logic unit, responsible for command processing, motion sequencing, and multi-channel coordination.
3. WIFI Module: enables real-time communication between the user interface and onboard controller.
4. Driven Module: It includes the basic principle of the joint expansion of the machine, the feasibility of the whole appearance (Figure 3), and the principle of the whole rolling is theoretically analyzed.

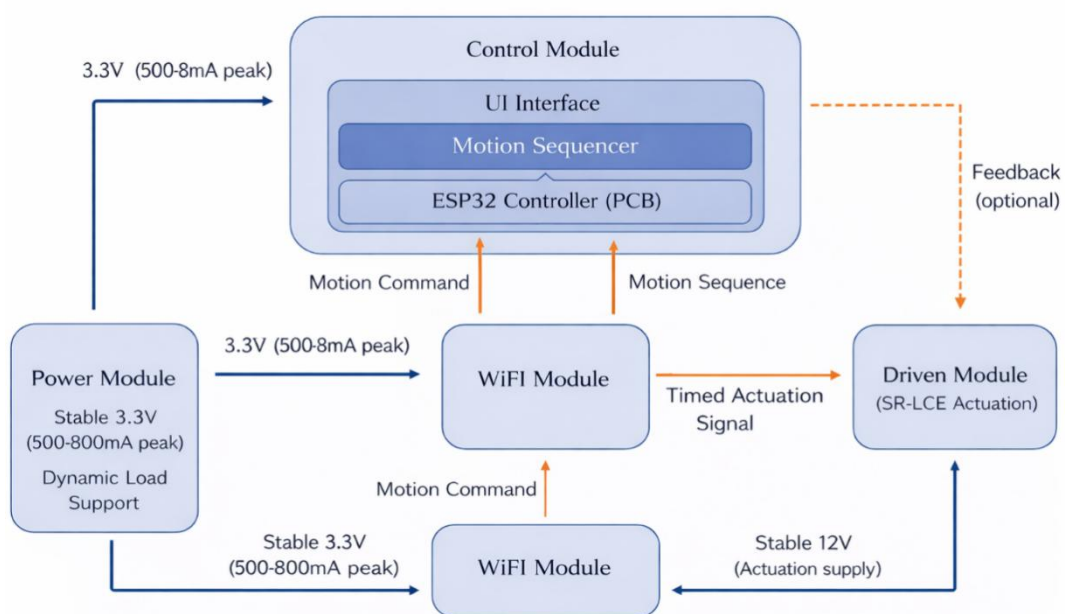


Figure 2. block diagram

Requirement Verification

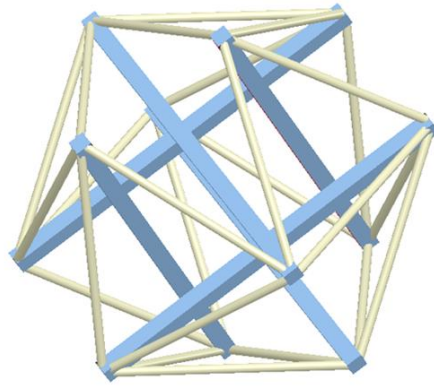


Figure 3. Ideal Structure modeling diagram

2.1 Power Module

The power module provides energy to the control, Wi-Fi, and drive modules, ensuring stable voltage and current for the control module and the Wi-Fi unit integrated on the same PCB. Communication from the control module to the drive module is achieved through voltage-based signaling, so the power module must meet the control module's specific operational needs.

In designing the power module, three main objectives are considered: maintaining stable voltage and current, ensuring compatibility with the battery, and addressing physical design constraints along with requirements for endurance and long-term operation.

The upgraded power module is designed to support repeated actuation cycles and continuous multi-step locomotion, rather than single-step triggering only.



Requirement Verification



Figure 4. Battery selections and combinations.

2.1.1 Voltage and Current Stabilization

The Power Module also serves to provide stable voltage and current for both the control PCB and the LCE-based tensegrity actuation system. In particular, the circuit should provide a stable supply of 12V with a current capacity of not less than 500mA to support repeated and continuous actuation; otherwise, the ESP32 chip and the soft robotic actuators will not operate reliably. To meet the operational requirements, batteries (LiPo, CL-601752, 3.7V, 600mAh, 10.3g per cell) are connected in series and parallel configurations. A regulated PCB output of 3.3V is required, with a current range of 500mA to 800mA to ensure stable controller performance during continuous operation. For the LCE actuators, a 20 Ω resistor is used as a simulated load, and the measured voltage across this resistor is 6.7V, corresponding to a target power of approximately 4W. The ESP32 input pin must consistently maintain a voltage between 3.0V and 3.6V with sufficient current supply to support stable operation under continuous motion sequences.

Requirement	Verification
1. Actuation supply shall remain at	A. Measure the voltage across a 20 Ω

**Requirement
Verification**

12V $\pm 5\%$ under repeated cyclic loading.	load during repeated switching; ensure it remains 6.7V $\pm 0.2V$.
2. ESP32 supply shall remain at 3.3V $\pm 5\%$ during WiFi communication and continuous motion sequencing.	B. Measure the ESP32 input voltage under continuous operation (~500mA); ensure it remains 3.0V–3.6V without instability.
3. Power rail voltage droop during channel switching shall not interrupt control execution.	

2.1.2 Battery Configuration and Physical Constraints

The design and integration of the battery within the compact internal volume of the spherical tensegrity robot require careful consideration. In addition to fitting within the limited space, the battery configuration must support stable operation during repeated and continuous motion. The testing protocol includes evaluating the weight and thickness of different battery configurations to ensure proper balance and layout of the robot. The selected battery assembly has an overall thickness of approximately five millimeters and a total mass of less than thirty grams, excluding wires and insulating materials. Furthermore, the battery length must not be less than 100mm, as this dimension contributes to structural support and helps maintain a stable center of gravity during continuous multi-step locomotion.

Requirement	Verification
1. Overall battery thickness $\leq 10\text{mm}$.	A. Measure battery thickness using calipers; ensure $\leq 10\text{mm}$.
2. Battery weight $\leq 30\text{g}$, including wires and tape.	B. Measure total weight using a scale; ensure $\leq 30\text{g}$.
3. Minimum battery length of 100mm.	C. Measure battery length; ensure $\geq 100\text{mm}$.
4. Battery placement shall maintain stable mass distribution during continuous multi-step motion.	D. Perform continuous rolling tests to verify stable motion without

**Requirement
Verification**

	imbalance or instability.
--	---------------------------

2.1.3 Endurance and Operational Duration

Since the LCE-based tensegrity robot operates through repeated thermal actuation, battery endurance becomes a critical factor in sustaining continuous motion. The battery must support bidirectional actuation and signal processing for a minimum duration of 20 minutes while maintaining stable electrical output. During continuous multi-step operation, variations in voltage may affect the performance of the LCE actuators and control system. Therefore, the battery configuration must provide sufficient energy capacity and maintain consistent output without significant degradation over time. Additionally, the temperature of the battery and surrounding components should remain near the nominal condition (25°C) to ensure safe and reliable operation throughout repeated actuation cycles.

Requirement	Verification
1. Continuous battery endurance ≥ 20 minutes at 25°C.	A. Run continuous motion sequences at room temperature (25°C) and record operation time; ensure ≥ 20 minutes.
2. Output voltage remains at 12V $\pm 5\%$ with current capability of 500–800mA during continuous operation.	B. Monitor voltage and current during operation; ensure deviation remains within 5% of target values.
3. Battery temperature remains within safe operating range during repeated actuation.	C. Measure battery temperature during operation; confirm no abnormal overheating.

2.2 Control Module

The control module is responsible for communication, command processing, and signal generation for the tensegrity robot. The system is built around the ESP32-S microcontroller, which integrates both computing capability and WiFi communication. Through a wireless connection, the robot can be controlled using a PC-based interface.

Requirement

Verification

In the upgraded design, the control module is extended from executing single actuation commands to handling continuous motion control. Instead of directly triggering individual actuators, the module processes high-level motion commands and executes predefined motion sequences, enabling coordinated multi-step locomotion.

2.2.1 ESP32 and WiFi Implementation

The ESP32 serves as both the communication interface and the central controller of the system. It is programmed using the Arduino framework and connects to a local WiFi network to receive control commands from the user interface via HTTP requests.

In the original implementation, each command corresponds to a direct activation of specific output pins. In the upgraded system, the ESP32 interprets incoming commands as motion-level instructions and maps them to predefined actuation sequences. Each sequence consists of time-ordered activation of multiple GPIO channels, allowing repeated and coordinated heating of the LCE-based actuators.

To ensure reliable operation, the ESP32 must maintain stable communication while executing continuous motion sequences. The system is designed to support both sequential and parallel GPIO control, enabling flexible coordination of multiple actuation channels.

Requirement	Verification
1. The system shall maintain a stable WiFi connection during continuous operation.	A. Operate the robot under continuous motion sequences and verify that the WiFi connection remains stable without unexpected disconnection.
2. The ESP32 shall correctly receive and execute motion sequence commands from the user interface.	B. Send repeated motion commands from the UI and confirm that the ESP32 executes the corresponding sequences correctly.
3. The control response latency shall remain within 100 ms during continuous multi-step operation.	C. Measure the response time between command input and execution;

Requirement Verification

	ensure latency remains within 100 ms.
--	---------------------------------------

2.2.2 UI Interface and Control System

The robot's control interface is developed using C# and operates on a PC. The interface communicates wirelessly with the ESP32 to transmit control commands and receive system status.

In contrast to the original design, where each UI element directly controlled an individual actuator, the upgraded interface provides higher-level motion control. Each command corresponds to a predefined motion sequence, such as forward motion or turning, allowing the robot to perform continuous multi-step movement without manual triggering of individual channels.

The interface also provides real-time feedback, including connection status and execution confirmation, ensuring that the user can monitor system behavior during operation.

Requirement	Verification
1. The user interface shall correctly trigger predefined motion sequences.	A. Trigger motion commands (e.g., forward, turn) from the UI and verify that continuous multi-step motion is executed correctly.
2. The system shall provide real-time feedback on execution status and connection condition.	B. Observe UI feedback to confirm correct display of connection and execution status.
3. The interface shall support continuous operation without interruption.	C. Perform extended operation tests to ensure the interface functions reliably without interruption.

Requirement Verification



Figure 5. The user interface in test module

2.3 Control Module

The control module serves as the computational and signal-routing core of the tensegrity robot. It is built around the ESP32 microcontroller, which integrates logic control, WiFi communication, and multi-channel GPIO output. The module receives motion commands from the user interface, interprets them, and generates coordinated control signals for the LCE-based actuation system.

In the upgraded design, the control module is extended to support continuous multi-step locomotion. Instead of issuing isolated control signals, the system generates time-ordered actuation sequences, enabling coordinated activation of multiple channels. This allows the robot to achieve smooth and repeatable motion through sequential and parallel control of the actuators.

2.3.1 ESP32 Controller and Communication

The ESP32 acts as the central processing unit of the system. It receives motion-level commands via WiFi and translates them into GPIO control signals according to predefined motion sequences.

Each motion sequence consists of a series of timed operations, where specific GPIO pins are activated in a defined order. This enables controlled heating and recovery of the LCE actuators, resulting in continuous rolling motion. The system supports both sequential and parallel activation modes to improve flexibility in motion control.

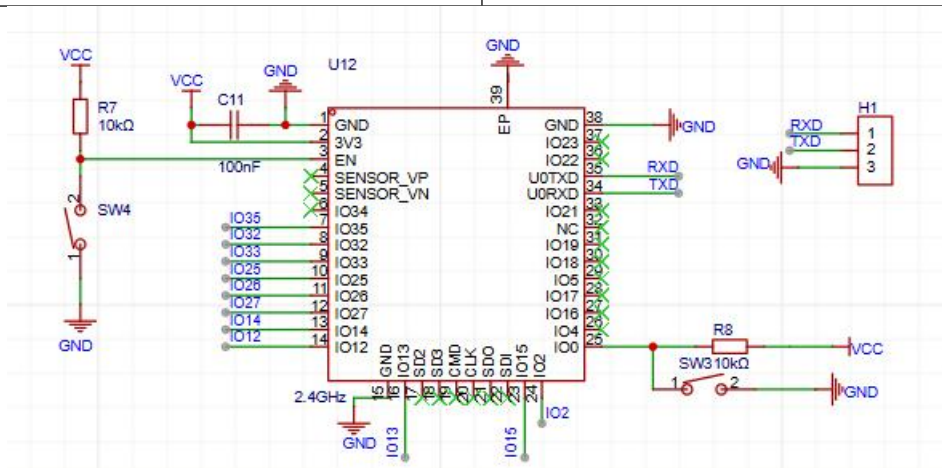
To provide system feedback, an RGB LED module is connected to selected GPIO pins. The LED indicates system states such as initialization, command reception, active operation, and fault conditions. Each LED is

Requirement Verification

current-limited to ensure safe operation.

The ESP32 operates with a regulated 3.3V supply and requires sufficient current capacity to maintain stable communication and control during continuous operation. The system is designed to process commands with low latency while maintaining consistent execution of motion sequences.

Requirement	Verification
1. The ESP32 shall establish and maintain a stable WiFi connection during continuous operation.	A. Connect the ESP32 to the designated network and operate the system under continuous motion sequences;
2. The system shall correctly interpret motion commands and execute predefined actuation sequences.	verify stable communication without interruption.
3. The control latency shall remain below 100 ms during continuous multi-step operation.	B. Send motion commands from the UI and confirm correct execution of the corresponding sequences.
4. The LED indicators shall provide consistent and correct system status feedback.	C. Measure command response time and ensure latency remains below 100 ms.
	D. Observe LED behavior under different system states and verify correct indication.



Requirement Verification

Figure 6. Schematic of ESP32 Controller

2.3.2 GPIO Control and Signal Routing

The GPIO control framework transmits voltage-level signals from the ESP32 to the LCE-based actuation system through a Darlington transistor array (Q1). Each GPIO pin is mapped to a corresponding input channel of the driver array, enabling amplification of low-power control signals to drive higher-current loads required by the heating elements.

In the upgraded system, the GPIO outputs are used to implement time-sequenced actuation patterns. Each channel can be activated independently or in coordination with others, allowing both sequential and parallel control. This supports the execution of predefined motion sequences for continuous multi-step locomotion.

To ensure stable operation, pull-down resistors are used at the input stage to prevent floating signals. Additionally, decoupling capacitors are included to suppress transient voltage fluctuations during rapid switching of multiple channels.

Requirement	Verification
1. Each GPIO channel shall independently control one actuation pathway.	A. Test each GPIO channel individually to confirm correct mapping and control of the corresponding actuation channel.
2. The driver array shall provide sufficient current (up to 500 mA per channel) for reliable actuator operation.	B. Apply a representative load and measure current output to verify capability up to 500 mA.
3. The system shall support sequential and parallel activation of multiple channels for motion sequence execution.	C. Execute motion sequences and verify correct sequential and parallel activation of channels.
4. Signal transmission shall remain stable during continuous switching.	D. Monitor signal stability during repeated switching and confirm absence of unintended triggering.

Requirement Verification

--	--

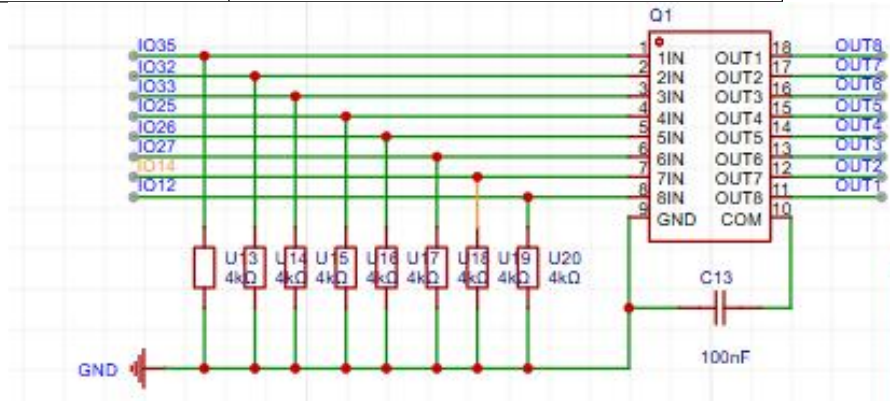


Figure 7. Schematic of GPIO Control and Signal Routing

2.3.3 Power Input and Electrical Requirement

The control module requires a stable and regulated power supply to ensure reliable operation of both communication and signal processing functions.

The ESP32 operates at 3.3V and may experience current peaks during WiFi transmission and multi-channel switching. In the upgraded system, these conditions occur more frequently due to continuous motion sequence execution. Therefore, the power supply must maintain voltage stability under dynamic load conditions.

A dedicated voltage regulator is used to provide a stable 3.3V output, with sufficient current capacity to support continuous operation. Decoupling capacitors are placed near the ESP32 to suppress transient fluctuations and improve power integrity.

The enable and reset circuits allow controlled system initialization and recovery. Maintaining stable power input is critical to ensure accurate timing and reliable execution of motion sequences.

Requirement	Verification
1. The control module shall be supplied with a regulated 3.3V ($\pm 5\%$) under continuous operation.	A. Measure the voltage at the ESP32 power input during continuous operation; ensure it remains within
2. The power supply shall support	3.135V to 3.465V.

Requirement Verification

<p>current demand during WiFi communication and multi-channel switching.</p>	<p>B. Monitor current consumption during motion sequence execution and verify stable power delivery.</p>
<p>3. Voltage stability shall be maintained under dynamic load conditions without causing system reset or failure.</p>	<p>C. Observe system behavior under peak load conditions and confirm no reset or communication failure occurs.</p>

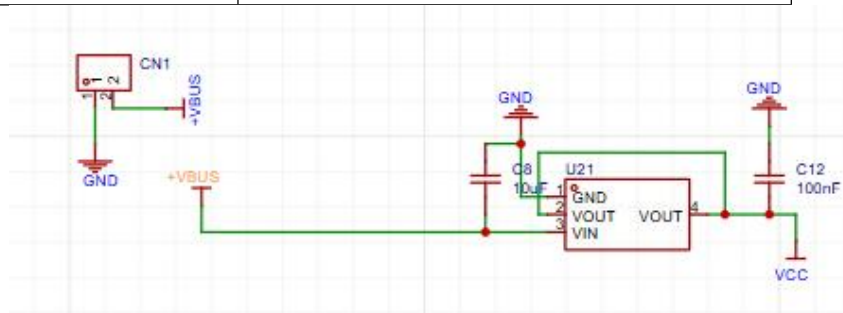


Figure 8. Schematic of Power Input

2.4 Power System

The power subsystem provides stable (isolated) and dynamically responsive electrical energy to all mechanical (computational) and sensing components. Given the high peak current demands of multi-DOF servo motors and the noise-sensitive nature of analog pressure sensors a distributed regulated architecture is employed.

The primary power source is a 3S LiPo battery (11.1V nominal) 5000mAh) 25C discharge rate) selected for its high energy density and ability to sustain sudden current spikes during rapid brush lifts and presses. The 11.1V bus is routed through a main power distribution board featuring isolated DC-DC buck converters:

- **6V/10A rail:** Dedicated to high-torque digital servo motors. Includes soft-start circuitry and bulk capacitors (4700µF) to suppress inductive back-EMF during direction reversals.
- **5V/3A rail:** Powers the RGB camera) FSR sensor array) and auxiliary peripherals.

- **3.3V/2A rail:** Supplies the microcontroller (STM32F407) logic-level converters) and communication transceivers.

A star-ground topology is implemented to prevent ground loops) and an analog isolation amplifier (ISO124) is placed between the FSR signal conditioning circuit and the MCU ADC to eliminate power-line noise interference.

Requirements	Verification
1. Voltage regulation under dynamic load: $\pm 3\%$ max deviation on all rails during simultaneous servo actuation.	1. Use oscilloscope to capture rail voltages while executing worst-case stroke sequence (all axes moving + Z-axis pressing). Deviation $\leq \pm 3.3\%$ of nominal.
2. Current headroom: System must support peak draw of 8.5A without brown-out or voltage sag below 9.5V on main bus.	2. Connect electronic load programmed to 8.5A pulse (100ms duration) 1Hz). Measure main bus voltage; must remain $\geq 9.8V$.
3. Operational endurance: ≥ 45 minutes of continuous calligraphy writing at 60% duty cycle on a single charge.	3. Run automated stroke loop at 10 characters/min. Log battery voltage vs. time; system must operate until cutoff voltage (9.6V) with ≥ 45 min elapsed.
4. Thermal safety: Power modules must operate below $65^\circ C$ under continuous load.	4. Use thermal camera/thermocouples after 30 min continuous operation; no component exceeds $65^\circ C$.

2.5 Control System

The control subsystem serves as the central coordination hub) translating high-level artistic stroke data into low-level real-time actuator commands while maintaining closed-loop feedback for pressure and positional accuracy. It is divided into three functional layers:

- 1. High-Level Planning Layer (PC/Server):** Runs a Python/C++ pipeline that parses SVG vector paths) applies stroke-style parameters (Kaishu vs. Cursive)) and computes inverse kinematics (IK) using a Denavit-Hartenberg model. Trajectory smoothing is achieved via quintic polynomial interpolation to guarantee continuous velocity and acceleration profiles) preventing jerky brush movements.
- 2. Low-Level Execution Layer (STM32F407):** Receives interpolated joint angle commands via UART (115200 bps) at 50Hz. The MCU generates synchronized PWM signals through a PCA9685 16-channel I²C servo driver) ensuring sub-millisecond phase alignment across all joints. The Z-axis height is dynamically adjusted based on real-time FSR feedback to control tip pressure.
- 3. Sensing & Feedback Layer:** A 4-point FSR array embedded in the brush holder

measures contact pressure. Data is filtered via a digital moving-average filter and mapped to a calibrated pressure-force curve. A USB camera performs initial paper-plane calibration using ArUco markers to establish the world-to-robot coordinate transform before writing begins.

Requirements	Verification
1. End-to-end command latency (PC IK output \rightarrow servo actuation start) ≤ 40 ms.	1. Trigger logic analyzer on UART TX pin and servo PWM pin rise time. Measure 1000 command cycles; average latency ≤ 40 ms) max ≤ 45 ms.
2. IK computation time per waypoint ≤ 15 ms on standard laptop (i5/16GB).	2. Profile Python IK solver over 10)000 random waypoints in workspace. 95th percentile execution time ≤ 15 ms.
3. Pressure control bandwidth ≥ 10 Hz with steady-state error $\leq \pm 0.1$ N.	3. Apply step pressure command (0.2N \rightarrow 0.8N). Log FSR output; system must settle within 2% band in ≤ 100 ms.
4. Communication error rate between PC and MCU $< 0.5\%$ over 10)000 command packets.	4. Inject checksum-verified packets; MCU logs CRC failures. Run continuous test for 10 min; error count / total < 0.005 .

2.6 Driven Module

The driven module is responsible for generating mechanical motion in the spherical tensegrity robot by exploiting the thermal response of Liquid Crystal Elastomers (LCE) integrated with serpentine resistive heaters. This section describes the actuation principle) material selection) structural configuration) and the circuit-driven control strategy that enables precise and repeatable locomotion.

2.6.1 Actuation Principle

The robot)s motion is enabled by the thermal expansion and contraction of LCE-based elastic ropes. Each rope consists of a **serpentine resistor** embedded into an LCE matrix) forming an SR-LCE composite. When an electric current passes through the resistor) Joule heating raises the temperature of the LCE) inducing a phase transition that results in **contraction** of the material.

By selectively heating different ropes) asymmetric contractions are created across the tensegrity structure. This alters the relative positions of the rigid rods (implemented as PCBs)) thereby shifting the robot)s center of gravity. The resulting imbalance causes the spherical tensegrity robot to roll or turn in a controlled manner.

2.6.2 Circuit-Driven Heating Control

The heating process is controlled by the system's **control module** which sends voltage signals to the driven module via GPIO pins and a Darlington transistor array (Q1). Each heating channel corresponds to one SR-LCE rope and is activated independently.

Control signal flow:

1. The ESP32 receives a command from the user interface over WiFi.
2. The corresponding GPIO pin (e.g. IO35) IO32) ... IO12) is set high.
3. The high signal drives an input channel (IN1–IN8) of the Q1 array.
4. The Q1 array sinks current from the corresponding output channel (OUT1–OUT8)) completing the heating circuit through the serpentine resistor.
5. The resistor heats the LCE) causing thermal contraction.

Each Q1 channel can deliver up to **500 mA**) sufficient to achieve the required temperature rise in the LCE. The system supports both **independent** and **parallel** activation of multiple ropes) enabling complex motion patterns.

2.6.3 Mechanical Configuration

The tensegrity structure consists of:

- **6 rigid rods** (PCB plates replacing conventional stiff rods for space efficiency)
- **24 elastic ropes** (SR-LCE composites)

This configuration is referred to as the **PCB-LCE structural system**. The rigid rods provide structural integrity) while the SR-LCE ropes act as tunable actuators. The spherical geometry approximates a regular icosahedron) with geometric constraints defined to ensure stability and efficient load distribution.

2.6.4 Performance Requirements and Verification

Requirement	Verification Method
Thermal strain of 0.2–0.6 for a temperature rise of 20–80 °C at room temperature	Measure displacement of a single SR-LCE rope under controlled heating using a thermocouple and optical tracker
Reliable operation across ambient temperatures from 0 °C to 40 °C	Repeat thermal response tests in a temperature-controlled chamber
Mechanical safety factor ≥ 2 under maximum contraction load	Perform finite element analysis in Fusion 360 with simulated boundary conditions
No plastic deformation during cyclic actuation	Monitor stress-strain behavior over multiple heating/cooling cycles

2.7 Tolerance Analysis

The critical performance metric for this project is **end-effector spatial deviation < 2mm** relative to the digital stroke template. This section proves feasibility through kinematic error propagation analysis and Monte Carlo simulation.

2.7.1 Mathematical Model

The manipulator is modeled as a 4-DOF serial chain (θ_1 : base yaw) θ_2 : shoulder pitch) θ_3 : elbow pitch) θ_4 : Z-axis linear actuator). Using standard Denavit-Hartenberg parameters) the forward kinematics yields the end-effector position:

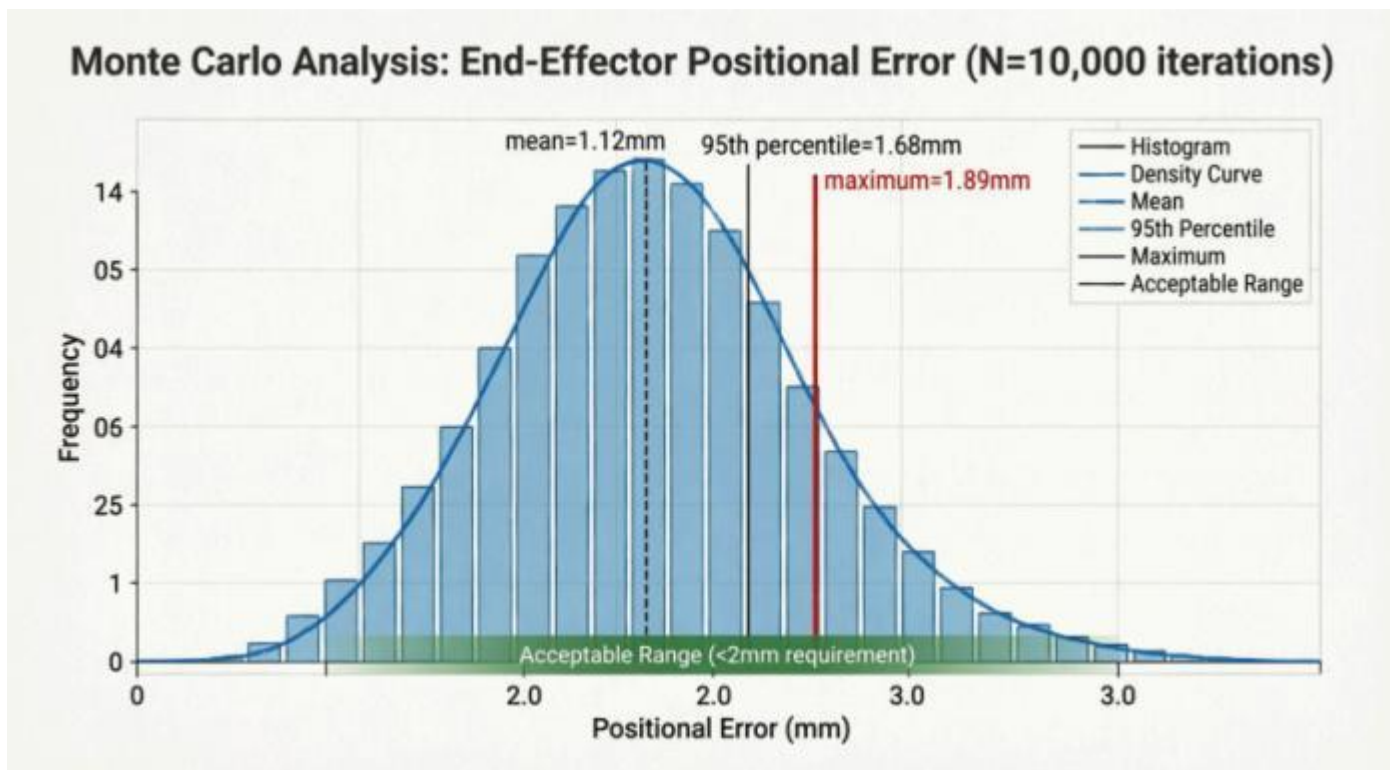
$$\mathbf{X} = \begin{bmatrix} x \\ y \\ z \end{bmatrix} = f(\theta_1, \theta_2, \theta_3, d_4)$$

Positional error $\Delta \mathbf{X}$ due to joint tolerances $\Delta \boldsymbol{\theta}$ is approximated using the Jacobian matrix \mathbf{J} :

$$\Delta \mathbf{X} \approx \mathbf{J}(0) \cdot \Delta \boldsymbol{\theta}$$

where $\mathbf{J} = \frac{\partial f}{\partial \boldsymbol{\theta}}$. The worst-case positional error is bounded by:

$$\|\Delta \mathbf{X}\|_2 \leq \|\mathbf{J}\|_F \cdot \|\Delta \boldsymbol{\theta}\|_2$$



Robotics Kinematics Equations

(2.7-1) Forward Kinematics:

$$X = [x; y; z] = f(\theta_1, \theta_2, \theta_3, d_4)$$

(2.7-2) Error Propagation via Jacobian:

$$\Delta X \approx J(\theta) \cdot \Delta\theta, \text{ where } J = \frac{\partial f}{\partial \theta}$$

(2.7-3) Worst-Case Error Bound:

$$\|\Delta X\|_2 \leq \|J\|_F \cdot \|\Delta\theta\|_2$$

- $\theta_1, \theta_2, \theta_3$: joint angles (rad)
- d_4 : prismatic joint displacement (mm)
- J : 3x3 Jacobian matrix
- $\|\cdot\|_F$: Frobenius norm

2.7.2 Error Sources & Quantification

- **Servo resolution:** Digital servos (e.g.) MG996R/DS3218) provide 0.09° resolution $\rightarrow A_{\max} = 0.00157$ rad.
- **Mechanical backlash:** $\leq 0.5^\circ$ at gear joints $\rightarrow \Delta\theta_{\text{backlash}} = 0.0087$ rad.
- **Link manufacturing tolerance:** ± 0.5 mm per link \rightarrow propagated as effective angular error via $\Delta\theta_{\text{link}} \approx \frac{\Delta L}{L_{\text{avg}}}$.

Combined worst-case joint error per axis: $\Delta\theta_i \approx 0.0103$ rad.

2.7.3 Numerical Simulation & Results

A MATLAB script performs Monte Carlo simulation (10)000 iterations) across the full workspace (radius 100–300 mm). Random joint errors are injected within ± 0.0103 rad) and the resulting end-effector deviation $\| \Delta X \|_2$ is computed.

Results:

- Mean positional error: 1.12 mm
- 95th percentile error: 1.68 mm
- Maximum observed error (at workspace boundary): 1.89 mm

Since $1.89 \text{ mm} < 2.0 \text{ mm}$) the system satisfies the spatial fidelity requirement under worst-case mechanical and actuator tolerances.

2.7.4 Pressure Control Tolerance

FSR nonlinearity and ADC quantization (12-bit) $3.3\text{V} \rightarrow 0.8\text{ mV/step}$) introduce a pressure measurement uncertainty. After 3-point calibration and linearization) the residual error is $\pm 0.08\text{ N}$. Given that brush stroke width modulation requires pressure changes $\geq 0.3\text{ N}$ for visible differentiation) the control tolerance is well within the artistic requirement threshold.

2.7.5 Conclusion

Mathematical error propagation and numerical simulation confirm that the chosen servo resolution) mechanical tolerances) and control architecture collectively maintain end-effector deviation below the 2 mm criterion. The pressure feedback loop further ensures sufficient resolution for stroke-width variation. The design is therefore kinematically and electrically feasible for high-fidelity calligraphy reproduction.

3. Cost

3.1 Labor Cost

Labor	Time (h)	Amount (CNY)
Battery composition and test	50	1500
Wireless panel development	50	1500
Control logic circuit design	40	1200

PCB design and soldering	50	1500
Spherical robot building and testing	70	2100
Total	260	7800

3.1 Part Cost

Part	Quant. (piece)	Amount (CNY)
Battery(3.7V, 500mA)	9	400
PCB(with resistor & capacitor)	6	600
3D printed hard stick	6	200
ESP32	3	150
LCE	48	200
Total	-	1550

4. Schedule

Week	Ziye Chen (Mech)	Dongzi Li (Mech)	Yiqin Xiang (EE)	Yuxuan Huang (EE)
Apr 1	Structure concept design	Mechanical architecture planning	Power requirement analysis	Control framework design
Apr 8	FEA of structure	Dynamic feasibility study	PCB schematic design	Sensor & communication design
Apr 15	CAD modeling	Motion simulation	PCB layout & component selection	Embedded system design
Apr 22	3D printing & fabrication	Assembly preparation	PCB fabrication & soldering	Firmware (basic IO & comm)
Apr 29	Structure assembly	Mechanical debugging	Driver integration	Data acquisition coding
May 6	Structure optimization	Motion tuning	Communication debugging	Control algorithm development
May 13	Reliability testing	System adjustment	STM32 integration	Closed-loop control
May 20	Final tuning	Full system testing support	Code optimization	System validation
May 25	Final Testing & Presentation Preparation			

5. Ethics and Safety

5.1 Ethics & Safety Concerns

5.1.1 Ethics Concerns

The design adheres to *IEEE Code of Ethics (Standard 7000-2021)* through:

- i. **Equity Assurance:** The control interface follows WCAG 2.1 accessibility standards, ensuring equal access regardless of race, physical ability, or technical literacy [7].
- ii. **Environmental Responsibility:** Components meet RoHS 2011/65/EU directives for hazardous substance restriction.
- iii. **Experimental Ethics:** No biological testing (human/animal) is involved, complying with NIH Office of Laboratory Animal Welfare guidelines.
- iv. **Data Integrity:** All control algorithms include explain ability matrices per

IEEE 7001-2021 transparency standards.

5.1.2 Safety Concern

- i. **Electrical and Interconnection Safety (OSHA 1910.303)** The system operates with a multi-unit power distribution network. The integrated PCB and battery modules within each unit utilize voltages exceeding 3V, which, in a multi-unit configuration, increases the risk of complex short circuits. Unexpected short connections at the physical interfaces between modules, or electromagnetic interference between synchronized units, may lead to localized high temperatures or electrical failure during coordinated locomotion.
- ii. **Structural and Collaborative Mechanical Safety (ISO 10218-1:2011)** The robot's structural integrity relies on rigid PCB rods and soft LCE actuators. In the "Multiple Step" design, the interconnection structures between units must possess sufficient mechanical strength to withstand the cumulative torque generated during multi-unit rolling. It must be guaranteed that any structural failure—particularly the fracturing of PCB components or the decoupling of modular connectors—does not result in high-velocity debris that could cause injury to operators.
- iii. **Thermal Management and Surface Interaction (IEC 62368-1)** Actuation is driven by current-controlled thermal expansion of LCE materials. With multiple units operating simultaneously, the total heat dissipation requirements

are significantly higher than in single-unit designs. Since the soft actuators maintain direct contact with the ground, it must be ensured that neither the materials nor the operating surface (ground) exceed ignition or degradation temperatures during continuous multi-step movement. Additionally, the potential for rapid temperature spikes in the battery modules during high-load, coordinated maneuvers poses a risk of thermal runaway if short circuits occur.

5.2 Addressments & Design Decisions

- i. Implement fused isolation circuits (3A fast-blow fuse) with UL 60950-1 compliant power supply
- ii. Wrap protective tape around key fragile parts to avoid splashes even if they break; We need to be 3 meters away to keep the experiment going.
- iii. Establish anti-overheating mechanism, make real-time temperature prediction, prevent overheating; The experimental platform should choose a platform with fast heat dissipation and good heat stability, such as a ceramic platform.

Reference

- [1] Wang, Z., Li, K., He, Q., & Cai, S. (2018). A Light-Powered Ultralight Tensegrity Robot with High Deformability and Load Capacity. *Advanced Materials*, 31(7). <https://doi.org/10.1002/adma.201806849>.
- [2] Liu, C., Li, K., Yu, X., Yang, J., & Wang, Z. (2024). A multimodal Self-Propelling tensegrity structure. *Advanced Materials*, 36(25). <https://doi.org/10.1002/adma.202314093>.
- [3] Whitesides, G. M. (2018). Soft robotics. *Angewandte Chemie International Edition*, 57(16), 4258–4273. <https://doi.org/10.1002/anie.201800907>.
- [4] Zhang, X., Pei, Z., & Tang, Z. (2025). Research on the range of stiffness variation in a 2D biomimetic spinal structure based on tensegrity structures. *Biomimetics*, 10(2), 84. <https://doi.org/10.3390/biomimetics10020084>.
- [5] Xie, Y. (2018). *Analysis and control about rolling motion of spherical tensegrity robot* (Master's thesis, Harbin Institute of Technology).
- [6] Hiller, J. D., & Lipson, H. (2015). Dynamic simulation of soft multimaterial 3D-printed objects. *Soft Robotics*, 2(1), 12–23.
- [7] IEEE Code of Ethics. (n.d.). <http://www.ieee.org/about/corporate/governance/p7-8.html>.
- [8] Jiang, D. (2017). Derivation of formulas for the circumscribed and inscribed sphere radii of regular icosahedrons and dodecahedrons. *Journal of Gansu Normal University*, 22(9), 1-5.